PAPER

CrossMark

Submarine and intertidal groundwater discharge through a complex multi-level karst conduit aquifer

Philip Schuler[1] · L. Duran[1] · T. McCormack[2] · L. Gill[1]

Abstract

The quantification of submarine and intertidal groundwater discharge (SiGD) or purely submarine groundwater discharge (SGD) from coastal karst aquifers presents a major challenge, as neither is directly measurable. In addition, the expected heterogeneity and intrinsic structure of such karst aquifers must be considered when quantifying SGD or SiGD. This study applies a set of methods for the coastal karst aquifer of Bell Harbour in western Ireland, using long-term onshore and offshore time series from a high-resolution monitoring network, to link catchment groundwater flow dynamics to groundwater discharge as SiGD. The SiGD is estimated using the "pollution flushing model", i.e. a mass-balance approach, while catchment dynamics are quantified using borehole hydrograph analysis, single-borehole dilution tests, a water balance calculation, and cross-correlation analysis. The results of these analyses are then synthesised, describing a multi-level conduit-dominated coastal aquifer with a highly fluctuating overflow regime draining as SiGD, which is in part highly correlated with the overall piezometric level in the aquifer. This concept was simulated using a hydraulic pipe network model built in InfoWorks ICM [Integrated Catchment Modeling]® version 7.0 software (Innovyze). The model is capable of representing the overall highly variable discharge dynamics, predicting SiGD from the catchment to range from almost 0 to 4.3 m^3/s. The study emphasises the need for long-term monitoring as the basis for any discharge studies of coastal karst aquifers. It further highlights the fact that multiple discharge locations may drain the aquifer, and therefore must be taken into consideration in the assessment of coastal karst aquifers.

Keywords Karst · Coastal aquifers · Tracer tests · Numerical modelling · Ireland

Introduction

Irish karst aquifers consisting of Carboniferous limestones, which are characterised by a low-lying topography and exposition to the coast, present a number of relevant research challenges, including groundwater flooding dynamics and the interaction of temporary flood lakes, i.e. turloughs (Naughton et al. 2012; Gill et al. 2013), saltwater intrusion (Perriquet et al. 2014), pipe network modelling in conduit-dominated catchments (Gill et al. 2013) and associated nutrient input into the aquatic coastal ecosystems (McCormack et al. 2014), and

submarine and intertidal groundwater discharge (SiGD; Cave and Henry 2011).

For karstic coastal catchments, strong heterogeneity must be expected (Burnett et al. 2006), which creates challenges in the application of methods to quantify dynamics. On the other hand, SiGD plays an important role in coastal ecosystems (Burnett et al. 2006), and therefore an understanding of its discharge dynamics is important. For example, nutrient loading via submarine groundwater discharge (SGD) driven by land use may enhance the development of toxic algae blooms (Silke et al. 2005) or harmful micro- or macroalgae (Green et al. 2014; Li et al. 2017a), or promote the over-development of certain fish species such as jellyfish (Dong et al. 2010). However, given the nature of the discharge locations, direct physical measurement of SiGD or purely SGD is not possible with the types of gauging methods used at onshore springs. Instead, studies have applied direct and indirect methods for measuring the mass transfer of groundwater across the sea floor (Zektser et al. 2007) or towards a surface water body, including (1) measuring the seepage flow rate using seepage

✉ Philip Schuler
   schulerp@tcd.ie

[1] Department of Civil, Structural and Environmental Engineering, University of Dublin Trinity College, Dublin 2, Ireland

[2] Geological Survey Ireland, Haddington Rd, Beggar's Bush, Dublin 2, Ireland

meters (Carr and Winter 1980; Corbett et al. 2003) or multi-level onshore piezometers (Freeze and Cherry 1979; Taniguchi and Fukuo 1996), (2) applying mass-balance approaches using natural geochemical tracers such as electrical conductivity (EC), short-lived radium and radon isotopes, i.e. ^{222}Rn, ^{223}Ra, ^{224}Ra, ^{226}Ra, or oxygen-18 (δ^{18}O) and deuterium (δ^2H) (Moore 2006; Peterson et al. 2008; Santos et al. 2008; Cave and Henry 2011; Lee et al. 2012; Null et al. 2014; Knee et al. 2016), (3) applying water balance approaches based on the contributing catchment (Sekulic and Vertacnik 1996; Smith and Nield 2003), (4) using hydrograph separation techniques to quantify the groundwater contribution of surface-water streams and extrapolating this contribution to the coastal shore (Zektser et al. 2007), (5) employing numerical modelling (Thompson et al. 2007; McCormack et al. 2014; Taniguchi et al. 2015), and (6) using thermal imaging from remote sensing (Johnson et al. 2008; Wilson and Rocha 2012; Tamborski et al. 2015). While methods 1–5 can be considered quantitative, method 6 by itself will only yield a purely qualitative result.

In Ireland, SGD has been known from ancient times, mainly associated with karstic limestones (Zektser et al. 2007). Due to the great tidal variation in the context of this study, SGD is defined as any input that is below the lowest ebb of spring tides (which is therefore typically > 4 m below sea level [mbsl]), whereas intertidal discharge occurs along the shore, influenced by tidal oscillation. While many spring locations draining as intertidal discharge are known, the discharge locations of purely SGD off the shore, presumably linked to lower sea levels during the Pleistocene (Drew 1990), are known to a lesser extent, although they are reported anecdotally by local fishermen and mariculture workers. SGD is linked to deeper flow paths in karst aquifers than in the case of intertidal discharge. Deep karstification with active groundwater flow is known to exist in Ireland relatively close to the shore, e.g. at 77 m below ground level [mbgl; approx. 67 mbsl (Mayol 2011)] or between 70 and 80 mbgl (approx. 60–70 mbsl), close to Kinvara on the western coast of Ireland, County (Co.) Galway (Cave and Henry 2011). It must be assumed that these low-lying conduits drain into the sea (Bunce and Drew 2017).

However, until recently, the discharge of coastal karst aquifers in Ireland has largely been conceptualised as intertidal discharge or shallow SGD close to the shore—for example, the Bell Harbour catchment in the Burren plateau located in the west of Ireland (Perriquet 2014; McCormack et al. 2017). Groundwater discharge into Bell Harbour bay is known to occur as submarine discharge as well as in the vicinity of intertidal springs, hence SiGD.

The purpose of this study is to improve the understanding of the hydrogeology of a complex coastal karst catchment in Ireland by combining different methods aiming to quantify SiGD, linked to understanding onshore groundwater flow dynamics by applying (1) a mass-balance approach in the form of a tidal prism model using specific EC records from seawater, (2) an onshore water balance for the assumed groundwater catchment of Bell Harbour, (3) single-borehole dilution tests (SBDT; Maurice 2009), (4) time-series analysis, and (5) a numerical pipe network model to simulate groundwater flow dynamics and SiGD into Bell Harbour bay.

This set of methods was combined to quantify SiGD, and further to explain the functioning of a complex coastal karst aquifer.

Materials and methods

Study area

The groundwater catchment of Bell Harbour (Fig. 1) forms the north-eastern part of the Burren limestone plateau located in the west of Ireland. The limestone massif of the Burren, including the upland catchment of Bell Harbour, is described as a temperate glaciokarst landscape, which was subject to repeated glaciation during the Pleistocene, showing features typical of glaciation such as ice-plucked crags, scoured rock surfaces, limestone pavements and erratic boulders (Simms 2014). Today's morphology of the catchment and the bay may be partly the result of glacial erosion during the last ice advance, whose direction is largely parallel to the bay (Drew 1990).

The catchment was delineated based on tracer tests previously executed in the region (Drew 2003). While the eastern and western boundaries are constituted by sharp escarpments and the northern boundary intersects with the shore, the extent of the catchment to the south is quite uncertain. Until now, no tracers injected in the southern part of the catchment have been recovered in Bell Harbour bay. The catchment covers at least 50 km^2 based on the topographical extent, but may extend further towards the south (Bunce and Drew 2017), potentially adding up to 13 km^2. The catchment is intersected by multiple valleys, with elevations ranging from sea level in the north to 300 m above sea level (masl) along the escarpments. Along the slopes the bare outcrop is uncovered, showing high degrees of karstification. In turn, in the valleys, relatively deep soil cover on outcrops of the limestone unit is attributed to Holocene weathering, forming the present erosion-resistant clay-rich soil (Moles and Moles 2002).

Due to the high degree of karstification, surface-water features are limited to short reaches of ephemeral streams, drainage from adjacent non-carbonate rocks, and turloughs (Drew 1990). Turloughs are described (EPA 2004) as topographic depressions in karst which are intermittently flooded on an annual cycle via groundwater sources and have substrate and/or ecological communities characteristic of wetlands. Within the catchment there are two turloughs (Fig. 1): Luirk
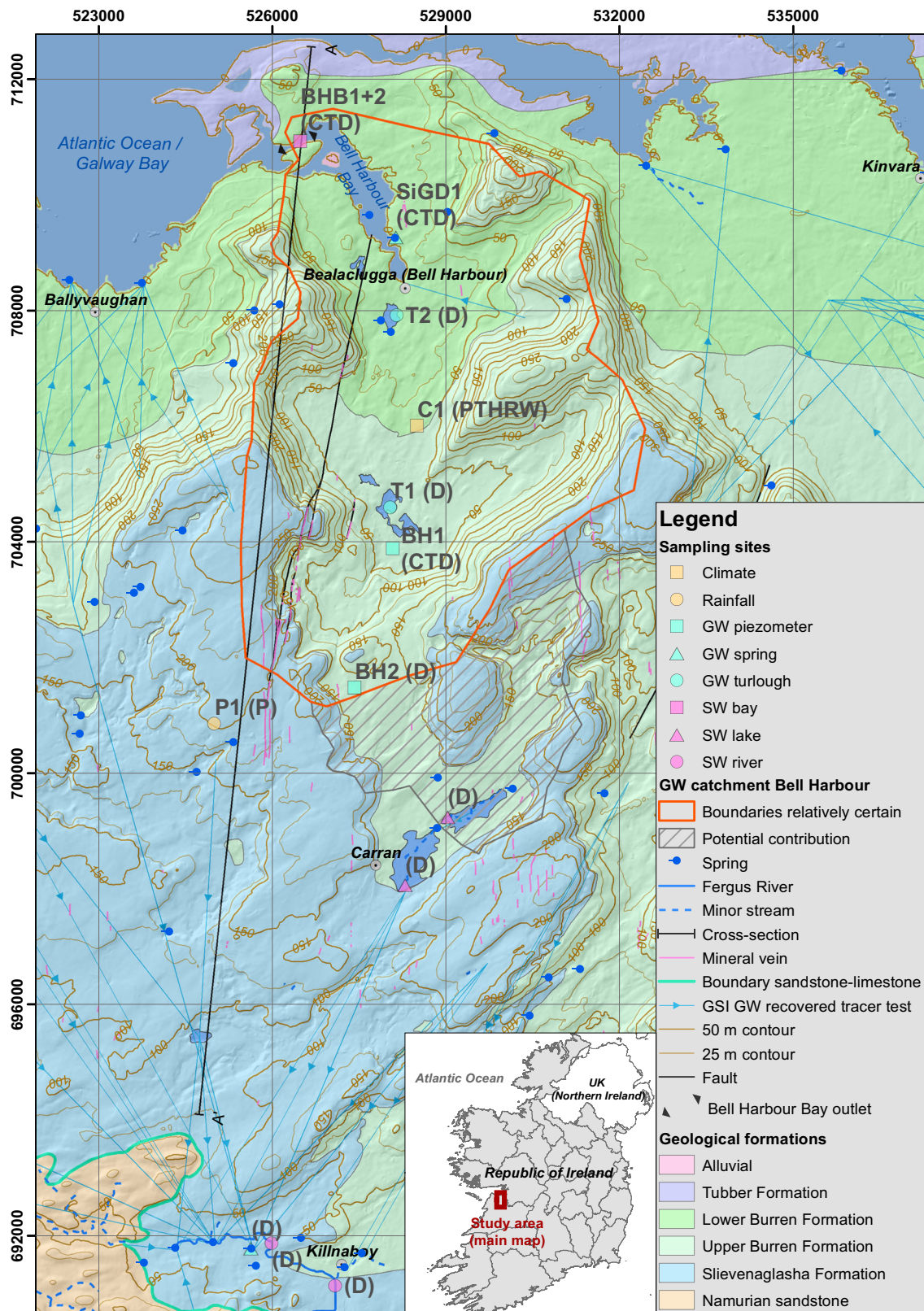
Fig. 1 Minimum groundwater catchment of Bell Harbour and potential additional contribution in the south in the Burren limestone plateau: topography, geology, structure, tracer tests, sampling locations (C = conductivity, D = depth, T = temperature, P = precipitation, H = relative humidity, R = net radiation, W = wind speed/direction). In the legend, GW is groundwater and SW is surface water

(T2) in the Lower Burren formation, and Gortboyheen (T1) within the Maumcaha formation.

Geology and structure

The entire catchment is underlain by Lower Carboniferous well-bedded and pure limestone ranging between the Tubber formation (early Viséan), the Lower Burren and Upper Burren formation (mid-Viséan, Asbian), and the Slievenaglasha formation (late Viséan, Brigantian), together reaching > 510 m in thickness above the Galway Granite. Dolomitic layers are known to exist at the top the Finavarra member (Pracht et al. 2004) and between the Lower Burren formation from the Upper Burren (Gallagher et al. 2006). Palaeokarst horizons occur at the top of the Maumcaha member below the overlying Aillwee member, which is distinguished between a Lower and Upper Aillwee member (MacDermot et al. 2003), and at the top of the Aillwee member. In addition, several impermeable clay "wayboards" are located within the Aillwee member, interpreted as palaeosols, which rest on irregular limestone surfaces considered to be palaeokarsts (Pracht et al. 2015). The dip of the strata is uniformly to the south, in the range of 2–3° (Fig. 2).

There is one fault in the catchment, i.e. MacDermot's fault in the western part of the study area, striking into the NNE sub-parallel to the Fergus Shear Zone, with a slight (< 200 m) sinistral displacement of members of the Burren and Slievenaglasha formations (Pracht et al. 2004). Joints strike NW–SE and E–W, and the age of joint formation is post-Variscan. The Variscan contractional deformation caused the formation of veins, which are laterally continuous and vertically consistent across bedding planes and discontinuities (Gillespie et al. 2001). Horizontal persistency of veins along strikes extends over 7 km, interconnecting caves (Mac Sharry 2006). Increased veining was recorded to depths of 204 –228 mbsl in the deep borehole drilled by the Geological Survey Ireland (GSI) at location BH1 (Fig. 1), as documented in the respective drilling log.

Hydrogeology

The hydrogeology of the catchment is largely influenced by erosion during the recent glacial advances as well as limestone dissolution. The groundwater flow is conduit-dominated from south to north, i.e. updip, as in the neighbouring catchment in the west, and the main groundwater discharge from the catchment is believed to have occurred via SiGD into Bell Harbour bay (Perriquet et al. 2012; McCormack et al. 2017). Bell Harbour bay has a very shallow topography, largely influenced by tidal oscillation: in the long term, 89% of water in the bay is drained during ebb tide. The main location of intertidal discharge is Pouldoody spring (SiGD1, Fig. 1), which is characterised by a high degree of fluctuation in EC, ranging

from <300 μS/cm during periods of high flow in winter to > 40,000 μS/cm during periods of low flow between spring and autumn. The assumption of a north–south flow direction along the dip can be ruled out, as there are no potential discharge locations for the catchment in the south. The south–north discharge pattern towards the bay allows for the possibility that preferential solution of the limestones would have taken place in the dominant south–north joints in the zone where fresh and saline water mix to produce subsaturated waters (Drew 1990). Minor and seasonal groundwater discharge occurs along the escarpment of the Aillwee member, where clay wayboards prevent vertical percolation and instead favour lateral flow above. However, clay wayboards are not continuous laterally, and can be locally intersected by vertically continuous dissolved mineral veins (Mac Sharry 2006), resulting in possible deep percolation. One example of the impact of veins on the hydrogeology is the development of Poll Gonzo cave from a dissolved vein that was explored between its top at 116 masl and the water table at 31 masl (Bunce 2010). Within the cave, laterally inflowing groundwater from the south travels rapidly downwards, and potentially further to the north into Galway bay (Bunce and Drew 2017).

The combination of the structural pattern and extensive erosion and dissolution caused the formation of conduits; the limestones of the Burren are classified as "regionally important karstified aquifers of conduit type" (GSI 2015). A shallow conduit following south–north within the valley was detected by McCormack et al. (2017). This conduit is assumed to connect the two turloughs in the valley, Gortboyheen (T1) and Luirk (T2), allowing the turloughs to rapidly fill following persistent periods of rain, and similarly to almost empty again.

Zones of deep karstification and high densities of perpendicular fractures were found in the deep borehole (BH1) at depths between 93 and 110 mbgl, corresponding to the sea level of the most recent ice age (McCormack et al. 2017).

The only mapped fault in the catchment, MacDermot's fault, shows evidence of being hydraulically active, as suggested by O'Connell et al. (2012).

Data

A monitoring network was established to continuously monitor climate, surface-water, and groundwater parameters (Fig. 1).

Groundwater level was measured (1) at two open uncased boreholes (BH1 and BH2) using an INW CT2X conductivity-temperature-depth (CTD) diver (Instrumentation Northwest, Inc. [INW], Kirkland, WA, USA), and (2) at the bottom of turlough Gortboyheen (T1) using a Schlumberger Mini-Diver (Schlumberger Water Services, BC, Canada). T1 is seasonally flooded while the measured water level represents the head in the underlying conduit system. SiGD was observed at the intertidal Pouldoody spring (SiGD1) using an INW CT2X
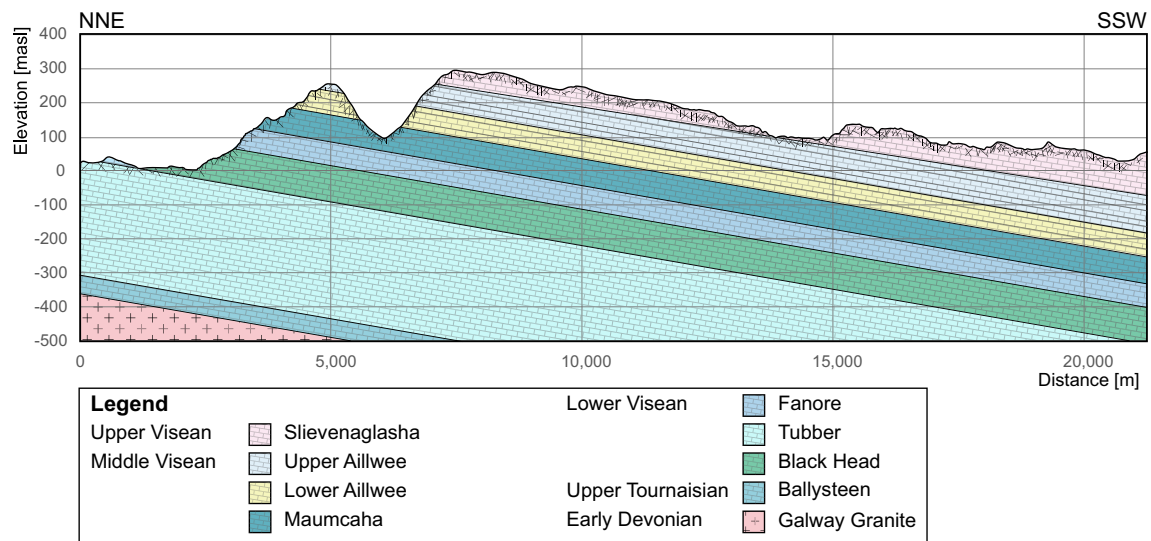
Fig. 2 Geological cross-section (A–A′, Fig. 1) through the catchment of Bell Harbour

CTD diver that was installed on a concrete platform placed at the shore.

A buoy sampler consisting of an anchoring bottom weight, a solid rope, and a floating buoy on the top was installed in the centre of the narrow outlet of Bell Harbour bay. The sampler was equipped with two sensors, BHB1 and BHB2 (INW CT2X CTD/Van Essen CTD-Diver [Van Essen Instruments, Delft, Netherlands]), at ~0.2 and 1 m below the water surface, respectively, continuously sampling specific EC, temperature (T), and depth at 10-min intervals. The instruments aimed to collect the abovementioned parameters during the incoming flood tide and outgoing ebb tide, of which EC was then used to quantify SiGD into the bay.

Rainfall and all relevant meteorological parameters for estimating the reference evapotranspiration according to the FAO-56 Penman–Monteith method (Allen et al. 1998) were sampled at the Burren Outdoor and Education Centre (C1) at ~38 masl, according to World Meteorological Organization guidelines (WMO 2008). A second rainfall sampler (P1) installed at ~203 masl on top of the Burren plateau showed the absence of a significant orographic impact on the rainfall regime, resulting in spatial heterogeneity.

All water levels were derived from pressure readings compensated to the barometric pressure measured continuously at C1 using an INW PT2X pressure sensor.

Secondary spatial data used for this study consist of the following: A 5-m bathymetric grid provided by the GSI was used to calculate the volume of the bay at different water levels. The bathymetric grid was combined with the Shuttle Radar Topography Mission (SRTM) elevation grid (USGS 2014) and complemented with data from extensive topographical field surveys using a Trimble 4700 (Trimble Navigation, Sunnyvale, CA, USA) differential global positioning system (GPS) with horizontal/vertical accuracy of 0.01 m, to derive

an improved 5-m elevation grid for the study area. This grid was used to calculate the volume of turloughs using ArcGIS (Esri, Redlands, CA, USA), followed by the establishment of a stage–volume curve for each turlough.

Cross-correlation analysis

In karst hydrology, cross-correlation (CC) has been used by several authors to characterise mostly input–output relationships between different time series (Padilla and Pulido-Bosch 1995; Angelini 1997; Larocque et al. 1998; Labat et al. 2000; Mathevet et al. 2004; Massei et al. 2006). For example, Larocque et al. (1998) demonstrated the usefulness of CC analysis on spatially distributed time series to characterise and delineate a karst aquifer according to common underlying dynamics.

In the present study, cross-correlation was carried out between rainfall, head levels in the borehole, turlough water level, and SiGD on the assumption that the time series could be regarded as bivariate stochastic processes that are stationary (Box and Jenkins 1976; Jukić and Denić-Jukić 2015).

Cross-correlation analysis was applied on hourly or daily time series of different monitoring sites to identify and quantify linear relationships between series to improve the understanding of catchment dynamics.

Single-borehole dilution tests

Ambient groundwater dynamics, including water level, temperature, and conductivity, were continuously measured in BH2 and BH1 using a CTD-Diver. In addition, single-borehole dilution tests (SBDT; Maurice 2009) were used to gain information on flow direction, mean flow velocities, and tracer recovery, as well as to locate inflow and outflow.

SBDT were conducted in BH1 under ambient, i.e. non-pumped, conditions following the method outlined by Maurice et al. (2011), applying concentrated emplacements of tracer solutions (125 g/l NaCl and deionised water) through a hose into the borehole, which was measured at the point of injection using a Schlumberger CTD-Diver (DI263), as well as above and below using a set of AquiStar® Aqua4PlusCT2X CTD (INW).

The total tracer recovery M_t [mg] was estimated by Eq. (1) (Field 2002):

$$M_t = \int_0^\infty C(t)\, Q(t)\, dt \tag{1}$$

with the tracer concentration C [mg/l] at time t [s] and the discharge Q [l/s]. The background total dissolved solids (TDS) concentration was accounted for.

The mean vertical travel time $\bar{v}$ [m/s] was calculated based on the mean residence time $\bar{t}$ [s], which is given by Eq. (2) (Field 2002):

$$\bar{t} = \frac{\int_0^\infty t C(t)\, Q(t)\, dt}{\int_0^\infty C(t)\, Q(t)\, dt} \tag{2}$$

Zones of inflow and/or outflow of groundwater were determined by repeating concentrated tracer injections after lowering or lifting the recording CTD diver, according to the direction of tracer plume migration from each previous test.

Quantification of SiGD

Quantification of SiGD into Bell Harbour bay was performed using continuously measured specific EC concentrations within the narrow outlet of the bay (BHB1 + 2) and applying a tidal prism model based on mass-balance principles (King et al. 2010).

For this study, a zero-dimensional (spatially uniform) modelling approach based on the repeated exchange of the intertidal volume was applied, based upon a pollution flushing model (Barber 2003; Barber and Wearing 2004). The model relates the water quality response of the bay to the external forcing effects of the tide, the initial pollutant loading, and the rate of groundwater discharge as inflow into the bay, i.e. SiGD. The model estimates the concentration of a conservative pollutant at the end of an ebb tide and the end of a flood tide. During the flood cycle, water from outside enters the bay and mixes with the existing water in the bay, including SiGD. During the following ebb cycle, the mixed bay water is drained outside the bay, and the concentration of a pollutant is estimated by the fundamental model equation, as Eq. (3):

$$C_{e(n)} = C_{f(n-1)} \exp\left\{ \frac{\pi Q_f}{\omega \sqrt{V_m^2 - V_t^2}} \right\} \tag{3}$$

where $C_{e(n)}$ is the pollutant concentration at the end of ebb tide n, $C_{f(n-1)}$ is the pollutant concentration at the end of the previous flood cycle, Q_f is the SiGD within the bay [m³], ω is the tidal angular frequency given by $\omega = 2\pi/T$, where T is the period of the tide [h], V_m is the mean volume of the basin [m³], and V_t is the amplitude of the oscillatory component of the tidal volume [m³].

In this study, the conservative pollutant was defined as the salinity of water represented, expressed as specific EC. Accordingly, the salinity in the bay results from incoming seawater during flood tide and dilution of seawater by SiGD into the bay. Given that SiGD into the bay could only be estimated during each ebb tide, Eq. (3) was rearranged to solve for Q_f to yield the SiGD at ebb tide n, as shown in Eq. (4):

$$Q_{(n)} = \frac{-2\sqrt{V_m^2 - V_t^2} \cdot \ln\left(\dfrac{C_{e(n)}}{C_{f(n-1)}} \right)}{\left(T_{e(n)} - T_{e(n-1)} \right)} \tag{4}$$

with the combined SiGD $Q_{(n)}$ [m³] of flood tide $n-1$ and ebb tide n at the end of each tidal cycle, the specific conductivity $C_{e(n)}$ [μS/cm] at the end of ebb tide n, the specific conductivity $C_{f(n-1)}$ [μS/cm] at the end of the previous flood cycle, and the time $T_{e(n)}$ at the end of the ebb tide n, as well as $T_{e(n-1)}$ at the end of the previous flood tide $n-1$.

The EC levels at the outlet of the bay were measured at two different levels to account for stratification, and combined to provide an average.

The combined time series was used to extract the minimum EC levels at the end of each ebb tide (C_e) and the maximum EC levels at the end of each flood tide (C_f). V_m was calculated using long-term tidal fluctuations measured at Galway Port (Marine Institute) and combined with 5-m bathymetry data (GSI) to yield a mean volume of Bell Harbour bay as 2.65 million m³. Accordingly, V_t was calculated as the standard deviation of long-term flood maxima and ebb minima, yielding 2.37 million m³.

Catchment water balance

The catchment water balance was applied according to Eq. (5):

$$P = \mathrm{GWR} + R + \mathrm{ET} + \Delta S \tag{5}$$

with the precipitation P, groundwater recharge GWR, runoff R, evapotranspiration ET, and change in storage ΔS. Since surface runoff is practically non-existent in the study area, R was considered to be zero. Changes in storage (notated by the ΔS) was accounted for by the dynamic water levels/volumes in the southern turlough (T1). The northern turlough (T2) was excluded from the calculation, as its absolute storage volume is negligible in this context.

Pipe network model

Based on the geometric architecture of the discrete conduit method (DCN; Thrailkill 1974; Jeannin 2001; Kovács and Sauter 2007), a pipe network model was developed to represent the hydrogeology of the catchment. While the DCN approach only accounts for groundwater flow in conduits or in connections between fractures, the semi-distributed pipe network model used here also includes additional diffuse groundwater recharge in interception catchments. Multiple groundwater flow dynamics and SiGD were modelled using InfoWorks ICM® version 7.0 commercial software (Innovyze, Tweed Heads, Australia), guided by principles outlined in Gill et al. (2013) and McCormack et al. (2017). The pipe model resembles diffuse groundwater recharge in permeable pipes modelled as laminar flow following Darcy's law, combined with the outline of major conduit flow horizons connected to the turlough (T1) on the surface, considering open channel and pressurised flow hydraulic conditions. The governing model equations for concentrated flow in the conduits are the Saint-Venant equations of conservation of mass and momentum, while the conveyance function was based on the Colebrook–White equation.

The catchment was divided into seven sub-catchments: three high-elevation sub-catchments with bare outcrop, three low-lying catchments with a soil cover, and the water surface of the bay outlet.

Mean elevations of each sub-catchment in the model were extracted from the improved digital elevation model. By doing so, the pipe network model realistically accounts for head differences between the low-lying centre and the surrounding escarpments, which is believed to add a driving force to the groundwater flow dynamics in the catchment.

As mentioned earlier (see "Data" section), uniform rainfall as measured at the two sites was applied on all sub-catchments. Climate variables were derived from the meteorological station at C1. Sea level time series were integrated into the model, based on values continuously measured at Galway Port (14 km north of the catchment) by the Marine Institute.

The model was calibrated against estimated groundwater recharge rates (Hunter Williams et al. 2013), water level fluctuations of the turlough Gortboyheen (T1), which is a function of the head in the underlying conduit, and estimates of SiGD into Bell Harbour bay. The modelling period was from 24 February 2016 to 15 July 2017.

Results

Borehole (BH1) hydrograph analysis

Figure 3 shows an example of the ambient borehole hydrograph at BH1 exhibiting a rapid response to rainfall and multiple recessions. It should be noted that there are no

pumps close to the borehole that could have an impact on the hydrograph.

During the first recession from 22 May to 10 June 2016, almost no rainfall occurred. Strikingly, the recession consists of multiple convex and concave sections, whereas the total hydrograph is split into two main recessions: above 20.2 masl [see (i) in Fig. 3a], and below 20.2 masl [see (ii) in Fig. 3a]. Below 16.5 masl, the recession is clearly influenced by tidal oscillation. The lagged correlation between the tidal amplitude and the borehole hydrograph in the beginning of June 2016 (Fig. 3) shows an oscillation pattern of ~6 h, with a delay of ±2 h at the borehole hydrograph.

The hydrograph of BH1 suggests:

- Water levels are highly fluctuating, ranging from 24 to 9 masl.
- The water level responds very rapidly to rainfall events, confirming that the borehole is hydraulically well connected to the aquifer.
- At least two distinct major recessions with changes from concave to convex sections are present—(1) > 20.2 masl, and (2) < 20.2 masl—suggesting the existence of multiple groundwater flow horizons.
- The water level oscillates in a frequency of 11–12 h below 16.5 masl. Lagged cross correlation between the tidal oscillation and BH1 yields a correlation coefficient of +0.08 and −0.10, for a lag of +3.5 h and −2.5 h, respectively, proving that BH1 is affected by the tidal fluctuation and is therefore connected to the sea.
- Head fluctuation is governed by rainfall as well as by the overall piezometric level in the aquifer, including the level in the turlough T1.

Hydrograph analysis shows that BH1 appears to be very well connected hydraulically to the main karst aquifer network. The recession is dependent on the piezometric level in the aquifer and in the turlough, clearly visible in the period from February to May 2016.

Single-borehole dilution tests

Twenty-three concentrated SBDTs were conducted in BH1 on six different days under different hydrological conditions using NaCl (125/62.5 g/l) and deionised water as tracer: campaigns 1 (11 Feb 2017), 2 (26 Feb 2017), 3 (4 Mar 2017), 4 (23 Mar 2017), 5 (14 Apr 2017), and 6 (13 Sep 2017). Deionised water was used to rule out the possibility that downward migration of NaCl tracer was density-driven.

Table 1 summarises the results of 19 successful tracer tests, including mean flow velocities and tracer recovery, considering the prevailing hydrological conditions. Single-tracer breakthrough curves are presented in Fig. 4. The prevailing flow direction during recessions was downwards (Fig. 4a–c),
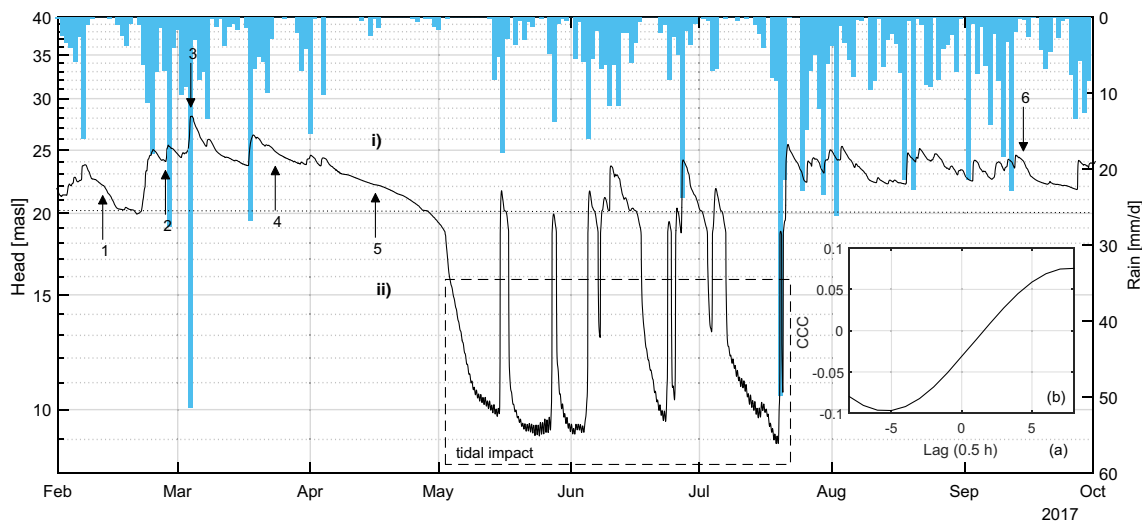
Fig. 3 a Ambient borehole recession at BH1 and daily rainfall between February and October 2017, showing rapid response to rainfall and multiple recessions which indicate different reservoirs. Numbers and arrows refer to tracer injections (single-borehole dilution tests). For the period from 17 July to 30 September 2017, rainfall data from the MetEireann station at Carron were used due to a data gap at C1. Areas (i) and (ii) are separated by the 20.2-masl level, which forms a significant break in the hydrograph recession. **b** Correlogram between the tidal oscillation (masl) and groundwater level (masl) of BH1 for 30-min (0.5-h) time series at low level. Although the cross-correlation coefficient (CCC) is relatively low, it does show a delay and impact of tidal oscillation on the borehole hydrograph. The hydrograph that is affected by the tide is highlighted in the dashed box

while just at the peak of a rising limb following a rain event, flow direction was upwards (Fig. 4d).

During tracer tests carried out on 4 March 2017, the groundwater flow direction was upwards. The low recovery rate of 0.1–0.3% is a clear indication of outflowing groundwater along the borehole section and associated loss of tracer.

Mean groundwater flow velocities were relatively high, reaching 263 m/h, confirming that the borehole must be well connected to highly transmissive fractures/conduits. Along the vertical borehole section, tracer was recovered between the top at 23.4 masl and the bottom at 176 mbsl.

In general, the groundwater flow direction was downwards, and tracer recovery and mean groundwater flow velocity decreased with increasing depth, suggesting continuous groundwater outflow along the depth of the borehole up to at least 176 mbsl (where tracer was still recovered).

The results highlight the presence of multiple highly conductive groundwater flow horizons, ranging from 23 masl to below 176 mbsl. It is therefore hypothesised that the groundwater flow regime in the catchment is largely influenced by a deep conduit, presumably draining groundwater as SGD. Surcharge of this deep channel, driven by heads from the surrounding escarpments, temporarily increases the head in BH1, activating more shallow conduits and draining as SiGD into the bay.

Quantification of SiGD

The borehole dilution test results (see "Single-borehole dilution tests" section) indicated the existence of a multi-level conduit system discharging the flows from the karst aquifer to the sea, with more intermittent SiGD into Bell Harbour bay via a shallow conduit system activated during periods of high recharge. Hence, in order to model the groundwater flow dynamics of this multi-level system, the balance between deep SGD and shallow SiGD needed to be estimated over varying hydrological conditions.

SiGD estimation was carried out according to the methodology in the "Quantification of SiGD" section, using continuous EC and tidal fluctuation measurements in the bay.

Figure 5a shows a plot of the resulting estimated averaged daily SiGD [m³/s] into Bell Harbour, indicating that the relationship between SiGD and rainfall is complex and non-linear. In spring 2016, SiGD reaches peaks of up to 3 m³/s, discharging 5.8 million m³ between 24 February and 28 April 2016. During summer and autumn 2016, the discharge into the bay clearly drops and largely varies between close to 0 and 0.6 m³/s, where even significant rainfall events do not appear to cause an increase in SiGD. In winter 2016, SiGD starts to increase again. During the period from 31 May 2016 to 15 July 2017, the total discharge accounts for 12.7 million m³, with a peak average daily discharge of 4.3 m³/s. Figure 5b shows the minimum and maximum EC values for all ebb and flood tides along with daily evapotranspiration at C1 using the Penman–Monteith equation. The higher EC amplitudes correspond to changes in EC between ebb and flood tide, which translates into higher SiGD (Fig. 5a). ET shows a typical seasonal trend—there is no obvious indication that ET influences EC amplitudes. Rather, EC amplitudes show rapid surges, such as in November 2016, which may be linked to the overall piezometric head in the aquifer (Fig. 5c).

Table 1 Summary tracer breakthrough curves of successful SBDT conducted in 2017 (see Fig. 4), including groundwater level, preceding rainfall (NA = not available) tracer injection depth, tracer sampling depth, tracer recovery, and mean groundwater (GW) flow velocity and flow direction (upwards ↑ or downwards ↓)

| Parameter		Date					
		11 Feb	26 Feb	4 Mar	23 Mar	14 Apr	13 Sep
Head (masl)		21.9	25.1	28.1	25.2	25.2	24.5
Number of injections (NaCl/deionised)		1/0	5/0	6/2	1/1	2/0	1/0
Preceding rainfall	12 h	0	24	1.6	0	1.4	NA
	24 h	0	24.4	37.8	0	1.4	1.9
	36 h	0	31	53	2.6	1.4	NA
	48 h	0	31.8	60	4.2	1.4	24.7
Tracer injection depth [masl]		−7	−4.3	+4.8	+4.8	+5.1	+4.8
Tracer sampling depth (range) [masl]		−16.9	−21.9 to −43.7	+18.4 to +23.4	−44.7	−80.4	−129.4 to −176
Tracer recovery (range) [%]		99.8	45.8 to 49.6	0.1 to 0.3	89.8	20.0	9.4 to 25.6
Mean GW flow velocity (range) [m/h]		185.0	146.3 to 156.7	198.0 to 262.9	54.7	89.0	43.3 to 97.0
Flow direction [↓/↑]		↓	↓	↑	↓	↓	↓

Rainfall remained fairly consistent throughout the period, with mean daily rainfall of 3.0, 3.4, 3.3, and 3.3 mm in spring, summer, autumn, and winter 2016/2017, respectively, and 3.1 mm in spring 2017; yet clearly the rate of SiGD decreased during the summer and much of autumn 2016. This observation is consistent with the continuous salinity measurements in the bay, which indicate very low variation in EC between the seawater entering during flood tide and water leaving during ebb tide in summer compared to spring and winter. The low rates of SiGD during summer and autumn 2016 suggest substantially reduced discharge from the intertidal springs in Bell Harbour bay. The discharge pattern of SiGD into Bell Harbour fluctuates considerably, suggesting the functioning of an overflow spring. This in turn implies that a significant quantity of groundwater from the catchment must also be draining to the sea, but bypassing Bell Harbour bay. The results in the "Single-borehole dilution tests" section suggest that such bypass flows are carried in much deeper conduits.

Fig. 4 Total dissolved solids (TDS) versus time. **a** Injection of 500 ml NaCl (62.5 g/l) at 4.3 mbsl, tracer recovery at 43.7 mbsl; **b** injection of 500 ml NaCl (62.5 g/l) at 4.3 masl, tracer recovery at 130.0 mbsl; **c** injection of 500 ml NaCl (62.5 g/l) at 4.3 masl, tracer recovery at 175.0 mbsl; **d** injection of 500 ml NaCl (125 g/l) at 4.8 masl, tracer recovery at 18.4 masl
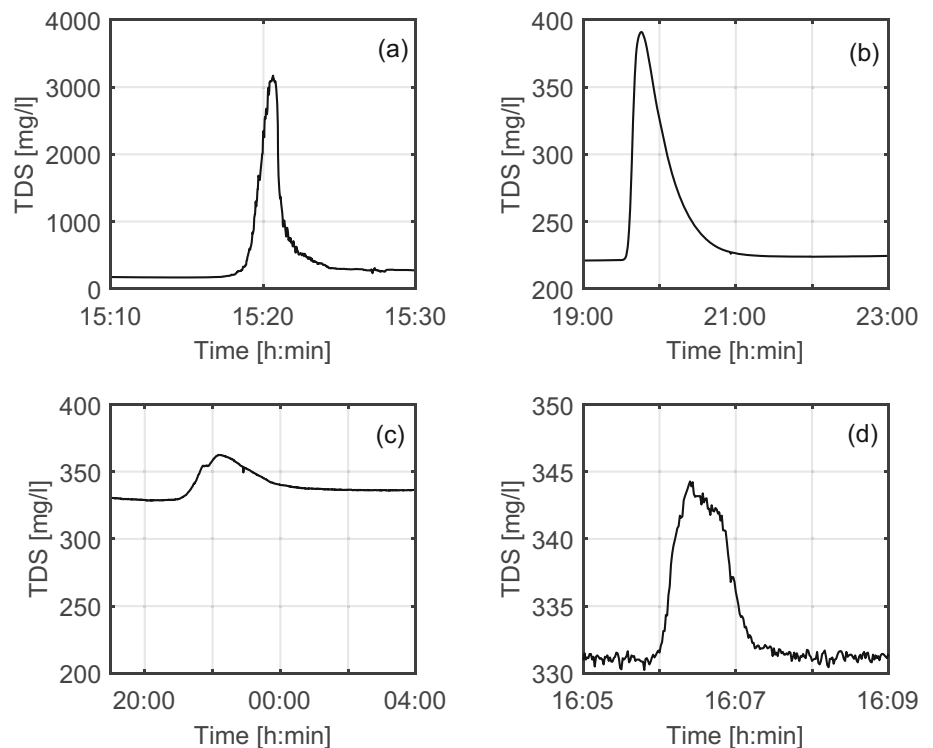
Fig. 5 a Estimated SiGD (m³/s) at Bell Harbour bay and rainfall (mm/day). Due to instrument malfunction, a data gap occurred for the period 28 April to 31 May 2016. **b** Minimum and maximum electrical conductivity values (EC, μS/cm) of ebb and flood tide and daily evapotranspiration (ET, mm) as measured at C1. **c** Hourly piezometric head (log scale) at BH1 (masl)
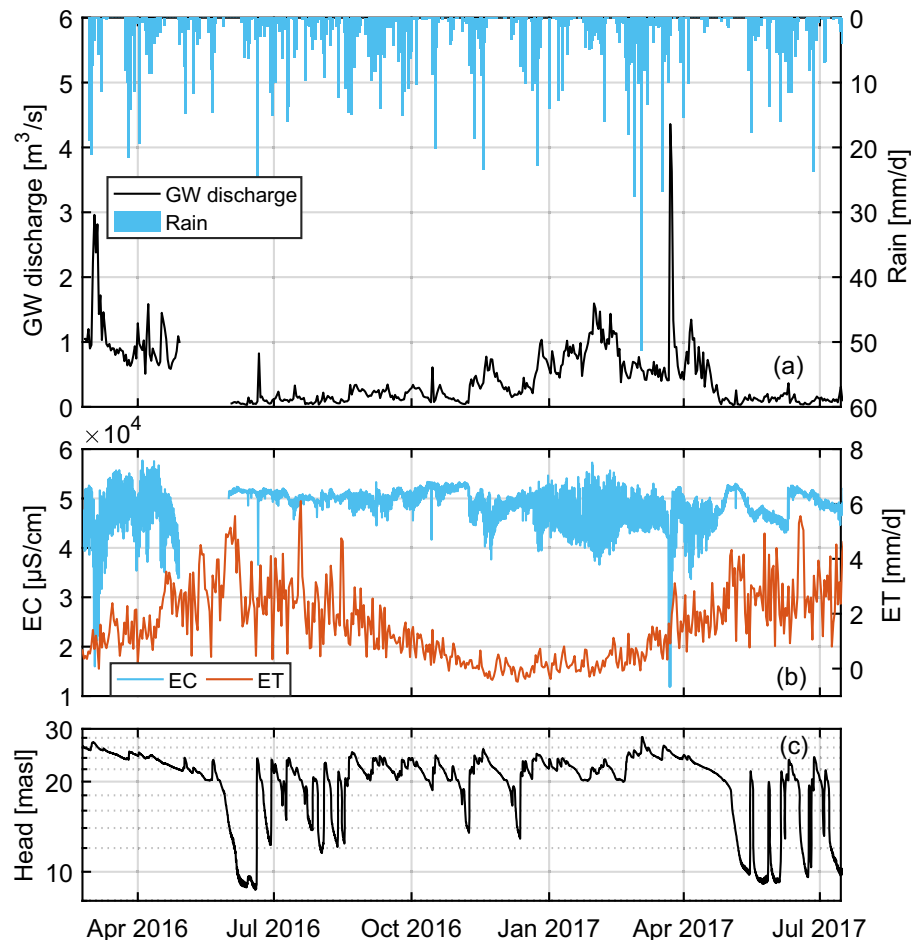

Cross-correlation analysis

While the previous three sections explained the complex pattern of time series from a single sampling location, cross-correlation was used to link individual time series in order to define common linear relationships as well as time lags between input time series (e.g. rainfall) and output time series (e.g. head). Cross-correlation coefficients (CCC) were calculated between hourly and daily time series, with the results mapped in Fig. 6. Since SiGD was estimated per tidal cycle, respective time series could only be cross-correlated for mean daily records. All other variables were cross-correlated using hourly time series. The results show a large variance in CCCs and lags, ranging from −0.21 to +0.87, and −54 h to +5 days, respectively.

Negative lags are calculated for the CCC between rainfall and BH2 (EC) and rainfall and BH1 (T). Because the respective relationships are one-directional, the negative lags suggest that other processes are involved (Jukić and Denić-Jukić 2015), where negative lags for the CCC between rainfall and EC and T in groundwater are not uncommon [e.g. Li et al. (2017b)].

The water levels in BH1 and BH2 respond to rainfall with a positive lag of 25 and 49 h, respectively; the significant lower lag time of BH1 suggests that the borehole is better connected to the aquifer than BH2. BH1 and BH2 are highly correlated, indicated by a CCC of +0.78 and a lag of −2 h, underlying the fact that the lowland BH1 responds before the upland BH2. While BH2 shows only a minor correlation with water levels in T1, water levels in BH1 and T1 are highly correlated (CCC = +0.84) by a lag of 0 h. This is not surprising, as BH1 and T1 are ~900 m apart, and it indicates that, indeed, BH1 must be very well connected to the karst aquifer, and its conduit system is also connecting the turlough.

In addition to the strong linear relationship between BH1 and T1, high CCC values were calculated between daily time series for BH1 and T1 and estimated SiGD into Bell Harbour bay, accounting for a CCC of +0.51 with a lag of 0 days, and even +0.87 with a lag of +1 day, respectively. The difference in lag may be explained by the inertia of the system: while the head in BH1 is a direct function of head within the aquifer, the water level in T1 does not respond linearly to the fluctuation in head within the aquifer. In fact, the turlough storage has much higher inertia, which is related to the depth–volume relationship of the turlough storage, whereby an increasing water

Fig. 6 Cross-correlation coefficients with lag times (h/day) in brackets for time series of rainfall (C1), borehole data (BH1, BH2), turlough level (T1), and estimated SiGD (BHB); D = depth, EC = electrical conductivity, P = rainfall, SiGD = submarine intertidal groundwater discharge, T = temperature. Arrows indicate the direction from input to output connecting the two sampling sites that the CCC and lag time refer to. DTM is the digital terrain model (topography)
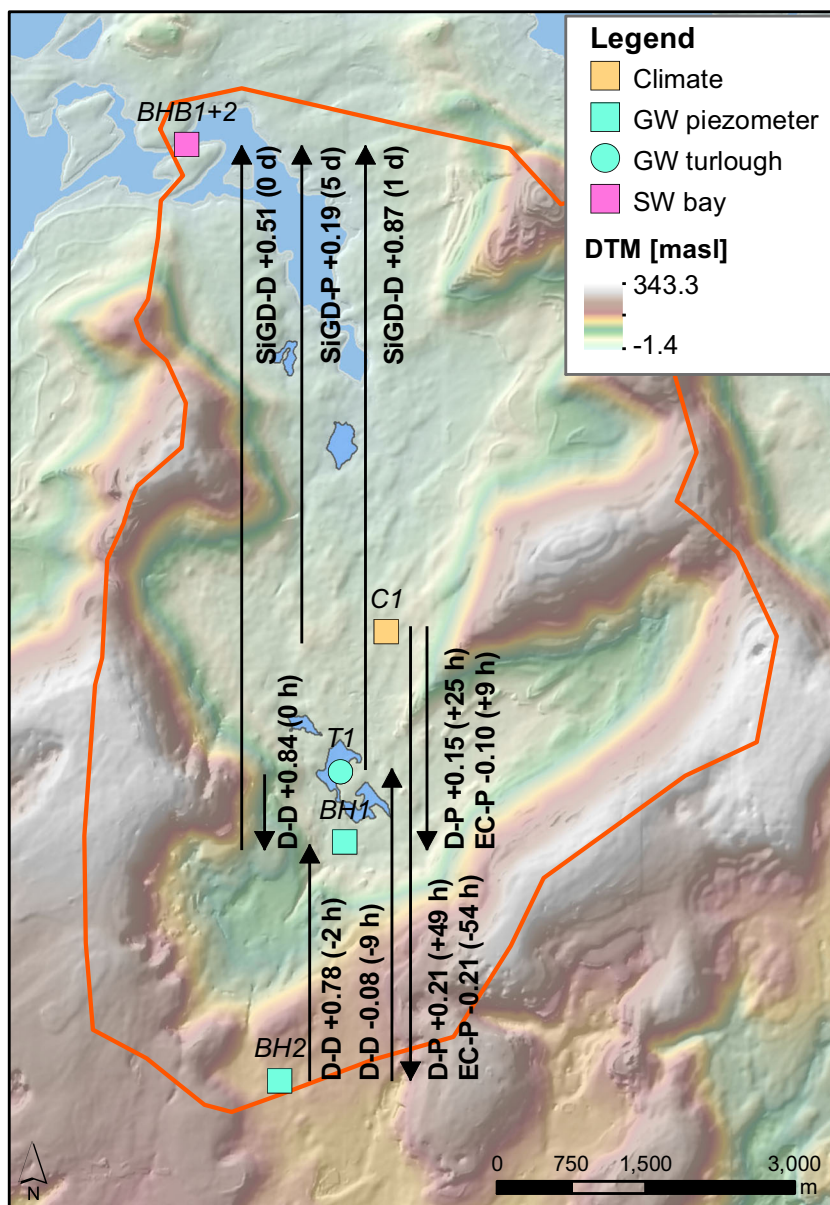
depth promotes an increasing surface area linked to the topography; the volume of water in the turlough is therefore not a linear function of its water depth. However, this result is particularly interesting, as it suggests a strong linear relationship between the head in the karst aquifer and the regime of SiGD into the bay.

Interestingly, CCC is high between BH2 and BH1, and between BH1 and T1, but not between BH2 and T1. This behaviour is interpreted as indicating that BH1 integrates two different dynamics that may govern the head in the aquifer: a slow-responding dynamic (overall piezometric state in the lowland) and a fast-responding dynamic (recharge dynamic in the upland). This interpretation would explain the lower lag between rainfall and BH1 (25 h) as opposed to rainfall and BH2 (54 h).

Water balance

Water balances have been used to match estimated SiGD to groundwater recharge in the catchment to quantify the share of groundwater that appears to bypass Bell Harbour bay via a deeper conduit system before being discharged as SGD further out into the sea.

Water balances for the catchment were established across two periods of differing recharge characteristics, i.e. winter (24 Feb to 28 Apr 2016, and 1 Nov 2016 to 31 Mar 2017, Fig. 7a, b) and summer (1 Jul to 31 Oct 2016, and 1 May to 16 Jul 2017, Fig. 7c, d), distinguishing between input (rainfall and turlough storage) and output (evapotranspiration, SiGD into Bell Harbour bay, and unaccounted resources). During the winter period, the catchment receives more rainfall overall,

which partially recharges turlough T1. SiGD accounts for 53 and 29% of total rainfall, and accordingly, the rate of unaccounted resources missing in the budget sums to 32 and 50% of total rainfall.

During the summer period, rainfall declines slightly, but most strikingly, the rate of SiGD drops to 8% of total rainfall for both summer periods. Accordingly, the rate of unaccounted resources is 68 and 69% of total rainfall.

The results underscore the large mismatch between total groundwater recharge and SiGD for the two seasons. The most plausible explanation based on this research in the hydrogeological context is that a significant share of groundwater must leave the catchment bypassing Bell Harbour bay via a deeper conduit flow system, draining the catchment continuously as SGD into the Atlantic Ocean. A higher rate of groundwater bypasses the bay in summer (68–69%) than in winter (32–50%).

It should be noted that the water balance estimations were calculated for the minimum size of the most probable catchment boundaries of 50 km^2. Any increase in the catchment boundaries, up to 13 km^2 larger, as displayed in Fig. 1, will increase total rainfall and ET in the calculation; however, SiGD in the calculation would remain constant, resulting in an increase in the contribution for unaccounted resources.

Pipe network model

The results presented previously led to the hypothesis of the functioning of both continuous SGD via a deep conduit into the Atlantic Ocean, and temporal SiGD into Bell Harbour bay via a shallow outflow. To verify the potential functioning of this flow regime, a pipe flow model was developed for the groundwater catchment based on the following findings (as outlined in previous sections):

- There is no strong linear relationship between the measured head in the aquifer and rainfall input, as indicated by the low CCC between rainfall and BH1 and BH2.
- The CCC between rainfall and BH1 and BH2, respectively, and CCC between BH2, BH1, and T1, respectively, suggest that at least two different dynamics are present, driving head differences between the lowland and the surrounding higher escarpments.
- SiGD varies throughout the year, showing a partly linear relationship with the water level measured at BH1 and a strong relationship to T1, providing evidence that the discharge pattern at least partly follows the head in the aquifer. During periods of high overall piezometric state of the aquifer, SiGD is activated through an overflow mechanism.
- The water balance for the groundwater catchment suggests that 32–69% of total rainfall is unaccounted for, including seasonal variation; it is believed this share of

water drains the catchment via SGD, bypassing Bell Harbour bay via a deep conduit.
- The borehole hydrograph recession of BH1 indicates the existence of multiple reservoirs and the impact of tidal oscillation on the borehole hydrograph at depths below 16.5 masl. Vertical groundwater flow directions are generally downwards, reaching below 176 mbsl, while flow direction changes to upwards during heavy rain events, driven by higher heads from the surrounding escarpments.

The multi-level karst groundwater flow system of Bell Harbour was thus modelled by a two-level pipe network model consisting of (1) a shallow network that ranges between 0 and 10 masl, discharging periodically as overflow SiGD into Bell Harbour bay, and (2) a deep conduit system at ~ 65 mbsl (~95 mbgl) bypassing Bell Harbour bay and discharging as SGD. In the absence of transmissivity data for the single groundwater flow levels, simplification of the system to two levels seems to achieve the most parsimonious model. Both levels are hydraulically connected with the conceptual model of the conduit network outlined in Fig. 8.
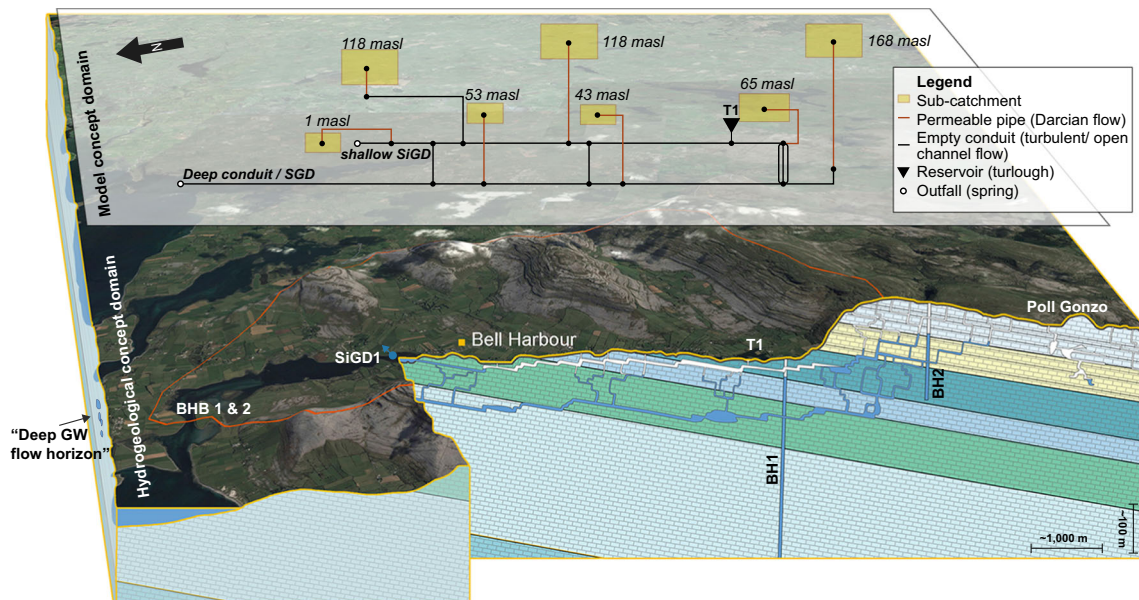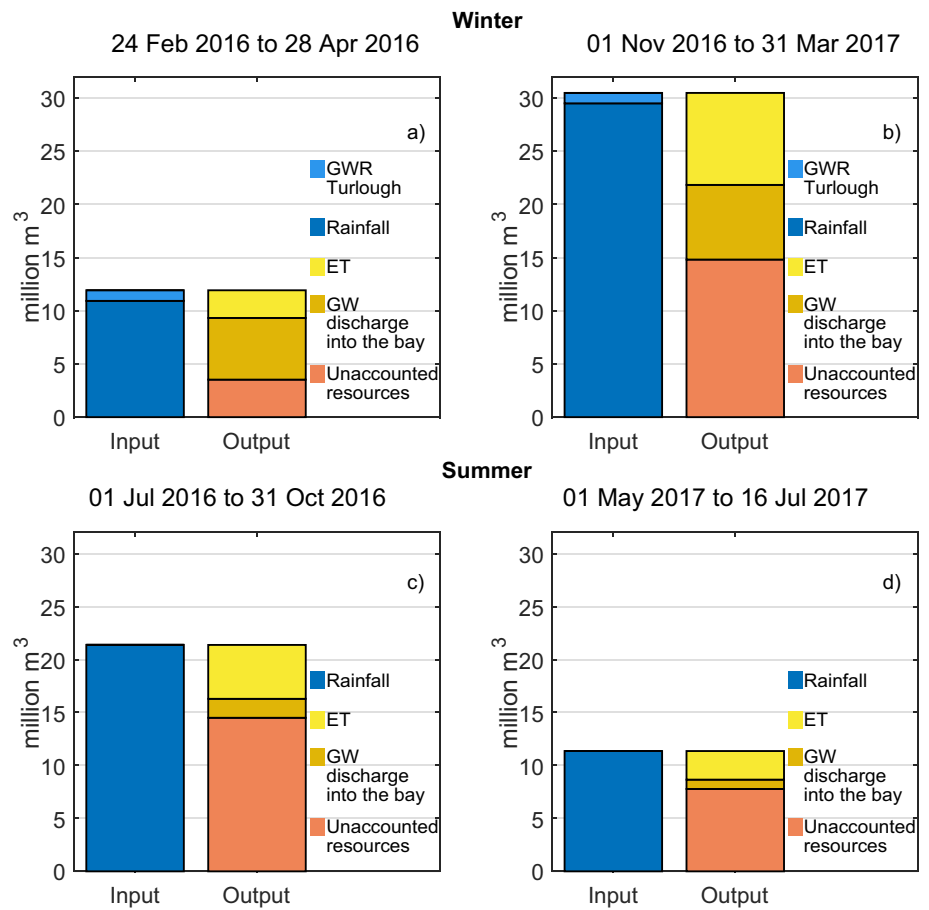
The southern, upper part of the catchment was calibrated against hourly water level time series of the turlough, T1 (Fig. 9). Due to restricted land access, data for T1 were only available until July 2016.

The model simulation was initiated during peak water levels in January 2016, after the beginning of available hourly rainfall data; therefore, the period for which T1 was calibrated could not extend beyond January to July 2016. Nevertheless, the result shows a very good fit between modelled water levels and observed levels, with a Nash–Sutcliffe (NS) coefficient of +0.99.

The modelled discharge of the shallow outflow was calibrated against previously estimated SiGD time series, which importantly involves different temporal resolution, i.e. (1) the model (1 h), and (2) the estimation of SiGD according to the occurrence of minimum/maximum EC records of the tidal cycle (11–14 h). The graphical analysis shows that the model is capable of modelling the overall discharge pattern: higher discharges in spring 2016, low discharge during the summer and autumn of 2016, increasing discharge in winter 2016, and again lower discharge in summer 2017. Furthermore, the decline in spring 2016 correlates with the decreasing head in T1.
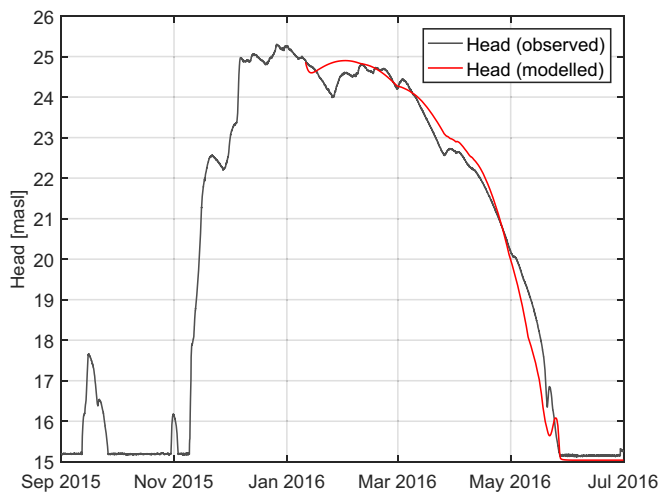
The absolute quantity of modelled SiGD matches the absolute estimated SiGD (Fig. 10): during period 1 (24 Feb to 28 Apr 2016), estimated SiGD was 5.9 million m^3, while simulated SiGD is 6.0 million m^3; in period 2 (31 May 2016 to 15 Jul 2017), estimated SiGD was 13.0 million m^3, which is matched by a simulated SiGD of 12.9 million m^3. There is a clear mismatch in January/February 2017, which cannot be directly explained. However, the instrumentation had become encrusted by that time, which may have trapped higher-EC water, making it potentially less responsive. Further, it can

Fig. 7 Water balances of Bell Harbour bay for (**a, b**) winter and (**c, d**) summer periods (million m^3)

Winter

24 Feb 2016 to 28 Apr 2016

a)

01 Nov 2016 to 31 Mar 2017

b)

GWR Turlough
Rainfall
ET
GW discharge into the bay
Unaccounted resources

Summer

01 Jul 2016 to 31 Oct 2016

c)

01 May 2017 to 16 Jul 2017

d)

Rainfall
ET
GW discharge into the bay
Unaccounted resources

Fig. 8 3D conceptual model of the hydrogeology, including conduit networks that resemble those in the pipe network model: permeable pipes (Darcy Flow) modelling diffuse recharge and empty pipes (open channel and turbulent flow) modelling conduit flow. Yellow boxes conceptually represent sub-catchments with mean elevations

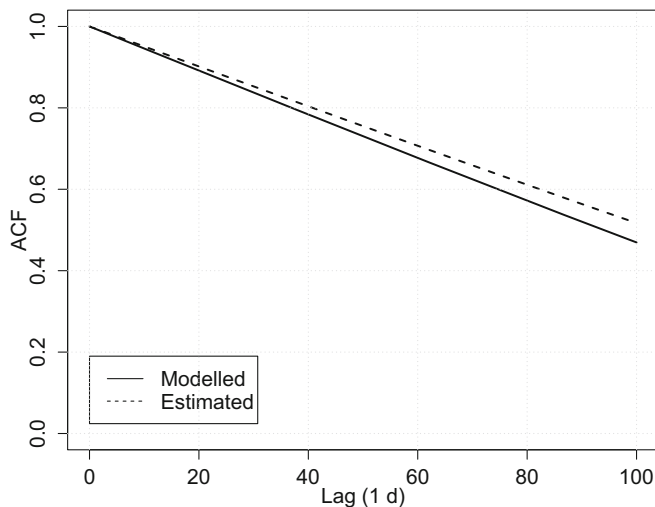Fig. 9 Modelled vs. observed turlough level (masl)

comparing the estimated and modelled SiGD, indicating reasonable model performance.

While the modelled turlough level achieves a good fit with the observed water level, the model performance is weaker between the modelled SiGD and estimated SiGD time series. This is not a surprise, since the tidal prism method of estimating SiGD is susceptible to errors according to some of the assumptions made, as well as the calculation time step of each "tidal cycle" of ~12 h acting to smooth out discharge peaks occurring in between. However, most importantly, the model simulates the general discharge pattern and single discharge peaks well, in addition to accurately predicting the estimated SiGD over both periods.

be hypothesised that abnormal currents strongly influenced the salinity at the monitoring site.

Comparison of time series of different temporal resolutions yields a loss in NS coefficient performance, especially when parameters derived from a longer time step were used for simulating flow with a shorter time step (Bastola and Murphy 2013). Therefore, the overall model performance was evaluated using average monthly SiGD rates, which yields an NS coefficient of +0.74, which can be considered "good" (Moriasi et al. 2007).

Further, the goodness of fit of the model results was evaluated using an autocorrelation function (Labat et al. 2000; Fig. 11). Overall, the loss in memory is very similar when

Discussion

This study presents a suite of methods, combined to create a novel approach for quantifying SiGD, and further for explaining the functioning of a complex coastal karst aquifer in Ireland. In this way, the study provides clear evidence for the existence of a multi-level coastal karst aquifer with very complex flow dynamics.

Hydrograph analysis of BH1 clearly suggests the existence of at least two sub-systems and the hydraulic connection of BH1 within the limestone aquifer, i.e. above 20.2 masl and below 20.2 masl. The latter sub-system is influenced by the tidal fluctuations, proving connection to the sea. The gradient between the onshore groundwater level at BH1 and the sea is

Fig. 10 **a** Modelled SiGD vs. estimated SiGD into Bell Harbour bay (m^3/s), and **b** cumulative modelled SiGD vs. cumulative estimated SiGD into Bell Harbour bay (million m^3) between 16 July 2016 and 15 July 2017

Fig. 11 Autocorrelation function (ACF) of modelled vs. estimated SiGD

sufficient to explain SGD: the lowest potential in BH1 reaches 9 masl, which means that, according to the Ghyben–Herzberg relation, the freshwater column at BH1 may reach a thickness of 360 m above potential seawater (Fleury 2005). The base level of the lower sub-system is not known; however, SBDTs prove vertical groundwater flow below 176 mbsl. Based on the SBDTs, groundwater flow is predominantly downward in BH1, with the gradient reversing only during flood peaks. This dynamic is believed to resemble the main principles of the aquifer: it is continuously drained via deep outlets discharging as SGD into the ocean. The occurrence of rain events causes a rapid increase in the potential head levels in the aquifer (Fig. 5c), yet, according to the relatively low CCC, rain is not the only variable driving head fluctuations. The low CCC between the piezometric head in BH1 and rainfall is believed to result from the influence of different hydraulic conductivities/transmissivities (heterogeneity) within the aquifer, as well as of the topography, i.e. the surrounding escarpments. Groundwater recharge in areas of higher elevation is thought to be the driving force for the short-term (~hours/days) increase in heads in BH1, resulting temporarily in upward groundwater flow in BH1 and flooding of T1. This behaviour was simulated using a pipe network model resembling a two-level conduit system, with a continuous outflow as SGD and an intermediate overflow as SiGD. The model is capable of simulating the impact of higher heads originating from the surrounding escarpments to model groundwater/surface-water interactions (i.e. turlough level fluctuations) and the seasonal pattern of SiGD into Bell Harbour bay. The pattern of SiGD into the bay shows a linear relationship with the head in the aquifer, as measured at BH1 and T1.

The findings regarding the functioning of the coastal karst aquifer raise questions and may be relevant for other studies in Ireland and worldwide. The development of coastal karst systems may be related to glaciation and glacial maxima, sea level changes, and tectonics, such as the

large-scale event of the Messinian salinity crisis which lowered the level of the Mediterranean to as much as 1500 m below the present level (Doerflinger et al. 2009). A result of that may be coastal karst aquifers with multiple outlet levels, such as Port-Miou in the Mediterranean (Fleury et al. 2007), which consists of a deep brackish conduit reservoir up to 223 mbsl and a shallow freshwater reservoir (Arfib and Charlier 2016).

As regards the last glacial maximum (LGM), 26 ka ago, the relative seawater level at the Irish coast has been modelled to 80–100 mbsl (Edwards and Craven 2017), while locally, at Galway Bay, a relative sea level was modelled to have dropped between 60 and 68 mbsl 15 ka ago (O'Connell and Molloy 2017). Older glaciation of comparable magnitude to the LGM occurred during the late Palaeozoic ice age, with onset indicated during the Late Viséan (Barham et al. 2012).

In comparison to the Mediterranean, the system of Bell Harbour in the Burren seems to be special, indicating multi-level conduits at depths greater than previously reported for the area (Smyth 2000), reaching below 176 mbsl. Interestingly, this depth exceeds the deepest sea level drop since the Pliocene. Therefore, there may be other factors that have influenced the formation of deep conduits, such as palaeokarst features, which may be linked to the Palaeozoic ice age and lowering of sea levels, or potentially dissolved mineral veins present in the catchment, as also suggested by Bunce and Drew (2017). Potential locations of SGD may be found in the Atlantic Ocean offshore at Ballyvaughan, as illustrated by Mullan (2003).

The present study introduces a novel technique for estimating SiGD in the form of a pollution flushing model (Barber 2003; Barber and Wearing 2004), which was supported by an extensive monitoring network that allows times series analysis, water budget estimations, and single-borehole dilution tests, to link onshore catchment dynamics to the offshore discharge pattern. Estimation of SiGD is challenging and is often reduced to single spot measurements or short periods of continuous observations (in the case of radon). However, this study emphasises the need to establish long-term time series that enable estimation of SiGD. Without such an approach, a highly fluctuating discharge regime cannot be assessed. Therefore, this study uses the natural tracer salinity, represented as EC, to quantify the SiGD into Bell Harbour. This was previously estimated by Perriquet (2014) using a tidal prism approach developed by Cave and Henry (2009). Interestingly, the lowest estimated discharge in the current study matches that in the previous work, which was found to be close to 0 m^3/s in May 2011. However, maximum discharge was estimated at ~23 m^3/s per tidal cycle, which is more than five times the estimated peak discharge in the present study. It has been suggested that the approach developed by Cave and Henry (2009) yields highly exaggerated estimates of

discharge rates (McCormack et al. 2014), which the present study would seem to corroborate.

By definition, a pipe network model is a simplification of the reality, while results suggest that dynamics of SiGD are driven by a multi-level conduit system with presumably different transmissivities, represented by a two-layer semi-distributed conduit system. This simplification may be one factor explaining the NS coefficient of +0.74. Another factor related to model performance is the time step of 1 h. The model was calibrated against hourly turlough water levels as well as the SiGD estimated per tidal cycle, represented by the period between the occurrence of minimum EC during ebb tide and maximum EC records during flood tide, ranging from 11.5 to 14 h. Therefore, the model was calibrated against time series of different temporal resolutions, reducing the model performance (Bastola and Murphy 2013). To account at least in part for this, the model was first calibrated to fit the 1-h turlough level fluctuations and was then further modified to fit the estimated SiGD time series.

The water balance approach has been used for the estimation of SGD in many places; yet the approach is typically imprecise for SiGD estimations, because uncertainties associated with values used in the catchments are often of the same magnitude as the discharge being evaluated (Burnett et al. 2006). For example, the delineation of the catchment boundaries is a critical aspect in karstified catchments (Margane et al. 2018). Additional uncertainty is added by using spatially uniform input data, such as rainfall, evapotranspiration, or salinity in the bay. However, in this study, the water balance approach is incorporated not to quantify the SiGD into Bell Harbour bay, but rather to argue in favour of the existence of SGD on a basin scale and to provide an estimate of deep groundwater flow.

Conclusions

Previously, the north-eastern part of the limestone Burren plateau was considered to drain almost exclusively via SiGD into Bell Harbour bay (Perriquet 2014; McCormack et al. 2017). The current study suggests that, in fact, the discharge pattern into the bay is driven by a complex overflow mechanism, depending on the overall piezometric potential in the karst aquifer. It has only been possible to investigate this overflow mechanism using a set of different methods that have not been applied before in this context, as well as long-term measurements of a dense onshore and offshore monitoring network:

- The existence of multiple groundwater flow horizons was indicated by a simple borehole hydrograph analysis showing different individual recessions, the lowest of which is clearly influenced by tidal oscillation, proving a connection between BH1 and the sea.

- The existence of deep groundwater flow was proven to exist using SBDT in BH1 that highlighted groundwater outflow from the borehole below 176 mbsl, as well as relatively high flow velocities according to the hydrological regime.
- Cross-correlation analysis established CCC values of +0.51 and +0.87 between the head in BH1 and SiGD, and the head in T1 and SiGD, indicating the partially linear relationship between the head in the aquifer and the SiGD regime.
- Water balances were established based on very conservative catchment boundaries, indicating a clear seasonal trend in the SiGD regime: during the two winter periods, SiGD accounted for 29 and 53%, while during the two summer periods, SiGD accounted for 8% only. This seasonal pattern reflects the role of the overall potentiometric head of the aquifer driving the discharge regime into Bell Harbour bay. Further, the results indicate that a large share of the groundwater must drain the catchment via unknown spring locations (32–69% of total rainfall).
- SiGD was estimated per tidal cycle using a relatively simple mass-balance tidal prism approach based on continuous measurements of EC for a period greater than 1 year. The resulting SiGD is a direct function of differences in EC between the flood and ebb tide, showing fluctuations in SiGD into Bell Harbour bay throughout the year.

The pipe network model is capable of simulating the periodic regime of SiGD characteristic of an overflow spring, as a function of the potentiometric head in the aquifer and matching the overall estimated SiGD for both periods of available data. Nevertheless, a mismatch between estimated and modelled SiGD in January and February 2017 raises the question of potentially unidentified flow paths that must be accounted for in the conceptual understanding of the catchment.

This study highlights the importance of long-term measurements for the assessment of (coastal) karst aquifers with complex or periodic discharge regimes. Further, it is argued here that in the context of coastal aquifers, different discharge locations may need to be considered in hydrogeological assessments in order to enable reliable quantification of the total discharge, as well other parameters of interest (such as nutrients), into the coastal zones.

References

Allen RG, Pereira LS, Raes D, Smith M (1998) Crop evapotranspiration—Guidelines for computing crop water requirements. FAO Irrigation and drainage paper 56, Food and Agriculture Organization of the United Nations, Rome

Angelini P (1997) Correlation and spectral analysis of two hydrogeological systems in Central Italy. Hydrol Sci J 42:425–438. https://doi.org/10.1080/02626669709492038

Arfib B, Charlier J-B (2016) Insights into saline intrusion and freshwater resources in coastal karstic aquifers using a lumped rainfall–discharge–salinity model (the port-Miou brackish spring, SE France). J Hydrol 540:148–161. https://doi.org/10.1016/j.jhydrol.2016.06.010

Barber RW (2003) Analytical modeling of pollution flushing in well-mixed tidal embayments. In: Lakhan VC (ed) Elsevier Oceanography Series. Elsevier, p 467–489

Barber RW, Wearing MJ (2004) A simplified model for predicting the pollution exchange coefficient of small tidal embayments. Water Air Soil Pollut Focus 4:87–100. https://doi.org/10.1023/B:WAFO.0000044789.67230.3e

Barham M, Murray J, Joachimski MM, Williams DM (2012) The onset of the Permo-Carboniferous glaciation: reconciling global stratigraphic evidence with biogenic apatite $\delta^{18}O$ records in the late Visean. J Geol Soc 169:119

Bastola S, Murphy C (2013) Sensitivity of the performance of a conceptual rainfall–runoff model to the temporal sampling of calibration data. Hydrol Res 44:484

Box GEP, Jenkins GM (1976) Time series analysis forecasting and control. Holden-Day, San Francisco

Bunce C (2010) Poll Gonzo. Ir Speleol 19:16–21

Bunce C, Drew D (2017) Water tracing in the Carran depression and River Fergus valley, Burren, Clare. Irish Groundwater Newsletter. Geological Survey Ireland, Dublin, p 13–18

Burnett WC, Aggarwal PK, Aureli A, Bokuniewicz H, Cable JE, Charette MA, Kontar E, Krupa S, Kulkarni KM, Loveless A, Moore WS, Oberdorfer JA, Oliveira J, Ozyurt N, Povinec P, Privitera AMG, Rajar R, Ramessur RT, Scholten J, Stieglitz T, Taniguchi M, Turner JV (2006) Quantifying submarine groundwater discharge in the coastal zone via multiple methods. Sci Total Environ 367:498–543. https://doi.org/10.1016/j.scitotenv.2006.05.009

Carr MR, Winter TC (1980) An annotated bibliography of devices developed for direct measurement of seepage. U.S. Geological Survey, Open-File Report 80-344, 37 pp

Cave RR, Henry T (2009) Groundwater inputs to the coastal zone of South Galway and Clare, west coast of Ireland. Paper presented at the ASLO Aquatic Sciences Meeting 2009, Nice, France

Cave RR, Henry T (2011) Intertidal and submarine groundwater discharge on the west coast of Ireland. Estuar Coast Shelf Sci 92:415–423. https://doi.org/10.1016/j.ecss.2011.01.019

Corbett DR, Cable JE, Shinn EA, Reich CD, Hickey TD (2003) Seepage meters and advective transport in coastal environments: comments on "Seepage Meters and Bernoulli's Revenge" by E. A. Shinn, C. D. Reich, and T. D. Hickey. 2002. "Estuaries" 25:126-132. Estuaries 26:1383-1387

Doerflinger N, Fleury P, Bakalowicz M, Ekmekci M (2009) Specificities of coastal karst aquifers with the hydrogeological characterisation of submarine springs – overview of various examples in the Mediterranean basin. Sustainability of the karst environment. Paper presented at the International Interdisciplinary Scientific Conference, Plitvice Lakes, Croatia, 23–26 September 2009

Dong Z, Liu D, Keesing JK (2010) Jellyfish blooms in China: dominant species, causes and consequences. Mar Pollut Bull 60:954–963. https://doi.org/10.1016/j.marpolbul.2010.04.022

Drew D (1990) The hydrology of the Burren, county Clare. Ir Geogr 23:69–89

Drew D (2003) The hydrology of the Burren and of the Clare and Galway Lowlands. In: Mullan G (ed) Caves of County Clare and South Galway. University of Bristol Spelæological Society, Bristol, p 31–43

Edwards R, Craven K (2017) Relative sea-level change around the Irish coast. In: Coxon P, McCarron S, Mitchell F (eds) Advances in Irish Quaternary Studies. Atlantis Press, p 181–215

EPA (2004) Guidance on the assessment of pressures and impacts on groundwater dependant terrestrial ecosystems, Risk Assessment Sheet GWDTERA2a – Risk to turloughs from phosphate. Water Framework Directive Pressures and Impacts Assessment Methodology, Guidance Document GW9. Working Group on Groundwater, Subcommittee on Turloughs.

Field MS (2002) The Qtracer2 program for tracer-breakthrough curve analysis for tracer tests in Karstic aquifers and other hydrologic systems. US Environmental Protection Agency, Washington, DC

Fleury P (2005) Sources sous-marines et aquifères côtiers méditerranéens. Fonctionnement et caractérisation (Submarine springs and Mediterranean coastal aquifers. Functioning and characterisation). Doctoral thesis, University of Paris

Fleury P, Bakalowicz M, de Marsily G (2007) Submarine springs and coastal karst aquifers: a review. J Hydrol 339:79–92. https://doi.org/10.1016/j.jhydrol.2007.03.009

Freeze RA, Cherry JA (1979) Groundwater. Prentice-Hall, Englewood Cliffs, NJ

Gallagher SJ, MacDermot CV, Somerville ID, Pracht M, Sleeman AG (2006) Biostratigraphy, microfacies and depositional environments of upper Viséan limestones from the Burren region, County Clare, Ireland. Geol J 41:61–91. https://doi.org/10.1002/gj.1033

Gill LW, Naughton O, Johnston PM (2013) Modeling a network of turloughs in lowland karst. Water Resour Res 49:3487–3503. https://doi.org/10.1002/wrcr.20299

Gillespie PA, Walsh JJ, Watterson J, Bonson CG, Manzocchi T (2001) Scaling relationships of joint and vein arrays from the Burren, Co. Clare, Ireland. J Struct Geol 23:183–201. https://doi.org/10.1016/S0191-8141(00)00090-0

Green L, Sutula M, Fong P (2014) How much is too much? Identifying benchmarks of adverse effects of macroalgae on the macrofauna in intertidal flats. Ecol Appl 24:300–314

GSI (2015) GSI Bedrock Aquifers 2015-06-16T00:00:00 - revision. Geological Survey Ireland, Dublin 2, Ireland. https://www.gsi.ie/Mapping.htm

Hunter Williams NH, Misstear BDR, Daly D, Lee M (2013) Development of a national groundwater recharge map for the Republic of Ireland. Q J Eng Geol Hydrogeol 46:493–506

Jeannin P-Y (2001) Modeling flow in phreatic and epiphreatic karst conduits in the Hölloch cave (Muotatal, Switzerland). Water Resour Res 37:191–200. https://doi.org/10.1029/2000WR900257

Johnson AG, Glenn CR, Burnett WC, Peterson RN, Lucey PG (2008) Aerial infrared imaging reveals large nutrient-rich groundwater inputs to the ocean. Geophys Res Lett 35:L15606. https://doi.org/10.1029/2008GL034574

Jukić D, Denić-Jukić V (2015) Investigating relationships between rainfall and karst-spring discharge by higher-order partial correlation functions. J Hydrol 530:24–36. https://doi.org/10.1016/j.jhydrol.2015.09.045

King JN, Mehta AJ, Dean RG (2010) Analytical models for the groundwater tidal prism and associated benthic water flux. Hydrogeol J 18:203–215. https://doi.org/10.1007/s10040-009-0519-y

Knee KL, Crook ED, Hench JL, Leichter JJ, Paytan A (2016) Assessment of submarine groundwater discharge (SGD) as a source of dissolved radium and nutrients to Moorea (French Polynesia) coastal waters. Estuar Coasts 39:1651–1668. https://doi.org/10.1007/s12237-016-0108-y

Kovács A, Sauter M (2007) Modelling karst hydrodynamics. In: Goldscheider N, Drew D (eds) Methods in karst hydrogeology. International Contributions to Hydrogeology 26, International Association of Hydrogeologists, Taylor & Francis, London, 264 pp

Labat D, Ababou R, Mangin A (2000) Rainfall–runoff relations for karstic springs. Part I: convolution and spectral analyses. J Hydrol 238:123–148. https://doi.org/10.1016/S0022-1694(00)00321-8

Larocque M, Mangin A, Razack M, Banton O (1998) Contribution of correlation and spectral analyses to the regional study of a large karst aquifer (Charente, France). J Hydrol 205:217–231. https://doi.org/10.1016/S0022-1694(97)00155-8

Lee CM, Jiao JJ, Luo X, Moore WS (2012) Estimation of submarine groundwater discharge and associated nutrient fluxes in Tolo harbour, Hong Kong. Sci Total Environ 433:427–433. https://doi.org/10.1016/j.scitotenv.2012.06.073

Li H, Zhang Y, Tang H, Shi X, Rivkin RB, Legendre L (2017a) Spatiotemporal variations of inorganic nutrients along the Jiangsu coast, China, and the occurrence of macroalgal blooms (green tides) in the southern Yellow Sea. Harmful Algae 63:164–172. https://doi.org/10.1016/j.hal.2017.02.006

Li Z, Xu X, Liu M, Li X, Zhang R, Wang K, Xu C (2017b) State-space prediction of spring discharge in a karst catchment in Southwest China. J Hydrol 549:264–276. https://doi.org/10.1016/j.jhydrol.2017.04.001

Mac Sharry B (2006) The influence of fractures on topography and groundwater flow in the Burren and Gort lowlands, western Ireland. Doctoral thesis, Trinity College, Dublin, Ireland, pp 259

MacDermot CV, McConnell B, Pracht M (2003) Bedrock Geology 1:100, 000 Sacle Map Series, Sheet 14, Galway Bay Geological Survey of Ireland, Dublin

Margane A, Makki I, Raad R, Schuler P, Abi-Risk J, Doummar J, Koeniger P, Hahne K, Stoeckl L (2018) Hydrogeology of the Jeita Groundwater Catchment in Lebanon. Geologisches Jahrbuch Reihe B Bundesanstalt fuer Geowissenschaften und Rohstoffe (BGR), Hannover, 192 pp

Massei N, Dupont JP, Mahler BJ, Laignel B, Fournier M, Valdes D, Ogier S (2006) Investigating transport properties and turbidity dynamics of a karst aquifer using correlation, spectral, and wavelet analyses. J Hydrol 329:244–257. https://doi.org/10.1016/j.jhydrol.2006.02.021

Mathevet T, Lepiller M, Mangin A (2004) Application of time-series analyses to the hydrological functioning of an alpine karstic system: the case of Bange-L'Eau-Morte. Hydrol Earth Syst Sci 8:1051–1064. https://doi.org/10.5194/hess-8-1051-2004

Maurice L (2009) Investigations of rapid groundwater flow and karst in the Chalk. Doctoral thesis, University College London

Maurice L, Barker JA, Atkinson TC, Williams AT, Smart PL (2011) A tracer methodology for identifying ambient flows in boreholes.

Groundwater 49:227–238. https://doi.org/10.1111/j.1745-6584.2010.00708.x

Mayol P (2011) Review of the South Galway Flood Study Report Office of Public Works, Headford, Co. Galway, p 43

McCormack T, Gill LW, Naughton O, Johnston PM (2014) Quantification of submarine/intertidal groundwater discharge and nutrient loading from a lowland karst catchment. J Hydrol 519, Part B:2318–2330. https://doi.org/10.1016/j.jhydrol.2014.09.086

McCormack T, O'Connell Y, Daly E, Gill LW, Henry T, Perriquet M (2017) Characterisation of karst hydrogeology in western Ireland using geophysical and hydraulic modelling techniques. Journal of Hydrology: Regional Studies 10:1–17

Moles NR, Moles RT (2002) Influence of geology, glacial processes and land use on soil composition and quaternary landscape evolution in the Burren National Park, Ireland. CATENA 47:291–321. https://doi.org/10.1016/S0341-8162(01)00190-4

Moore WS (2006) Radium isotopes as tracers of submarine groundwater discharge in Sicily. Cont Shelf Res 26:852–861. https://doi.org/10.1016/j.csr.2005.12.004

Moriasi DN, Arnold JG, Van Liew MW, Bingner RL, Harmel RD, Veith TL (2007) Model evaluation guidelines for systematic quantification of accuracy in watershed simulations. Trans ASABE 50:885–900

Mullan G (2003) Caves of County Clare & South Galway. University of Bristol Spelological Society, Bristol, 259 pp

Naughton O, Johnston PM, Gill LW (2012) Groundwater flooding in Irish karst: the hydrological characterisation of ephemeral lakes (turloughs). J Hydrol 470–471:82–97. https://doi.org/10.1016/j.jhydrol.2012.08.012

Null KA, Knee KL, Crook ED, de Sieyes NR, Rebolledo-Vieyra M, Hernández-Terrones L, Paytan A (2014) Composition and fluxes of submarine groundwater along the Caribbean coast of the Yucatan peninsula. Cont Shelf Res 77:38–50. https://doi.org/10.1016/j.csr.2014.01.011

O'Connell Y, Daly E, Duffy GP, Henry T (2012) Investigation of submarine groundwater discharge and preferential groundwater flow-paths in a Coastal Karst area using towed Marine & Terrestrial Electrical Resistivity. Paper presented at the American Geophysical Union Conference, San Francisco, 3–7 December 2012

O'Connell M, Molloy K (2017) Mid- and late-Holocene environmental change in western Ireland: new evidence from coastal peats and fossil timbers with particular reference to relative sea-level change. Holocene 27(12):1825–1845. https://doi.org/10.1177/0959683617708447

Padilla A, Pulido-Bosch A (1995) Study of hydrographs of karstic aquifers by means of correlation and cross-spectral analysis. J Hydrol 168:73–89. https://doi.org/10.1016/0022-1694(94)02648-U

Perriquet M (2014) Characterization of the hydrodynamics and saltwater wedge variations in a coastal karst aquifer in response to tide and precipitation events (Bell Harbour catchment, Co. Clare, Ireland). Doctoral thesis, National University of Galway, Ireland

Perriquet M, Henry T, Cave R, Leonardi V, Jourde H (2012) Hydrodynamics of a coastal karst aquifer affetced by saltwater intrusion under oceanic climatic influence, Co. Clare, Ireland. Paper presented at the 22nd Salt Water Intrusion Meeting, Búzios, Brazil, 17–22 June 2012

Perriquet M, Leonardi V, Henry T, Jourde H (2014) Saltwater wedge variation in a non-anthropogenic coastal karst aquifer influenced by a strong tidal range (Burren, Ireland). J Hydrol 519:2350–2365. https://doi.org/10.1016/j.jhydrol.2014.10.006

Peterson RN, Burnett WC, Taniguchi M, Chen J, Santos IR, Ishitobi T (2008) Radon and radium isotope assessment of submarine groundwater discharge in the Yellow River delta, China. J Geophys Res Oceans 113:C09021. https://doi.org/10.1029/2008JC004776

Pracht M, Lees A, Leake B, Feely M, Long B, Morris J, McConnell B (2004) Geology of Galway Bay: a geological description to

accompany the Bedrock Geology 1:100,000 map series, Sheet 14, Galway Bay Geological Survey of Ireland, Dublin

Pracht M, Somerville ID, Wang Y (2015) A revised Mississippian lithostratigraphy of county Galway (western Ireland) with an analysis of carbonate lithofacies, biostratigraphy, depositional environments and palaeogeographic reconstructions utilising new borehole data. J Palaeogeogr 4:1–26. https://doi.org/10.3724/SP.J.1261.2015.00065

Santos IR, Niencheski F, Burnett W, Peterson R, Chanton J, Andrade CFF, Milani IB, Schmidt A, Knoeller K (2008) Tracing anthropogenically driven groundwater discharge into a coastal lagoon from southern Brazil. J Hydrol 353:275–293. https://doi.org/10.1016/j.jhydrol.2008.02.010

Sekulic B, Vertacnik A (1996) Balance of average annual fresh water inflow into the Adriatic Sea. Water Res Dev 12:89–97

Silke J, O'Beirn FX, Cronin M (2005) Karenia mikimotoi: an exceptional dinoflagellate bloom in Western Irish Waters, Summer 2005. Marine Environment and Health Series No. 21, Marine Institute, Galway

Simms MJ (2014) Karst and Paleokarst☆. In: Reference Module in Earth Systems and Environmental Sciences. Elsevier, p 1–10

Smith AJ, Nield SP (2003) Groundwater discharge from the superficial aquifer into Cockburn sound Western Australia: estimation by inshore water balance. Biogeochemistry 66:125–144. https://doi.org/10.1023/B:BIOG.0000006152.27470.a9

Smyth T (2000) A case study in the Gort/Ardrahan area of South Galway. In: Gendreau N (ed) FLOODaware Final Report. European Commission, p 163-171

Tamborski JJ, Rogers AD, Bokuniewicz HJ, Cochran JK, Young CR (2015) Identification and quantification of diffuse fresh submarine groundwater discharge via airborne thermal infrared remote sensing. Remote Sens Environ 171:202–217. https://doi.org/10.1016/j.rse.2015.10.010

Taniguchi M, Fukuo Y (1996) An effect of seiche on groundwater seepage rate into Lake Biwa, Japan. Water Resour Res 32:333–338. https://doi.org/10.1029/95WR03245

Taniguchi M, Ono M, Takahashi M (2015) Multi-scale evaluations of submarine groundwater discharge. Proc. IAHS 365:66–71. https://doi.org/10.5194/piahs-365-66-2015

Thompson C, Smith L, Maji R (2007) Hydrogeological modeling of submarine groundwater discharge on the continental shelf of Louisiana. J Geophys Res Oceans 112:C03014. https://doi.org/10.1029/2006JC003557

Thrailkill J (1974) Pipe flow models of a Kentucky limestone aquifer. Groundwater 12:202–205. https://doi.org/10.1111/j.1745-6584.1974.tb03023.x

USGS (2014) Shuttle Radar Topography Mission (SRTM) 1 Arc-Second Global. USGS EarthExplorer. https://earthexplorer.usgs.gov/

Wilson J, Rocha C (2012) Regional scale assessment of submarine groundwater discharge in Ireland combining medium resolution satellite imagery and geochemical tracing techniques. Remote Sens Environ 119:21–34. https://doi.org/10.1016/j.rse.2011.11.018

WMO (2008) Guide to meteorological instruments and methods of observation, 8th edition. World Meteorological Organization, Geneva

Zektser IS, Dzhamalov RG, Everett LG (2007) Submarine groundwater. CRC Press, Boca Raton, pp 466